Water Based Frequency Selective Surface Acting as an Absorber

Water Based Frequency Selective Surface Acting as an Absorber

Catalin Pescari[1], Andrei-Marius Silaghi[1], Aldo De Sabata[1], Ladislau Matekovits[1,2,3]
[1] Department of Measurements and Optical Electronics, University Politehnica Timisoara, Timisoara, Romania
catalin.pescari@upt.ro, andrei.silaghi@upt.ro, aldo.de-sabata@upt.ro
[2] Department of Electronics and Telecommunications, Politecnico di Torino, Torino, Italy
[3] Istituto di Elettronica e di Ingegneria dell'Informazione e delle Telecomunicazioni, National Research Council of Italy, 10129 Turin, Italy
ladislau.matekovits@polito.it

***Abstract*— Absorbers are used for selective enclosure screening and stealth technology. This paper proposes a cost-effective frequency selective surface (FSS) that functions as a narrow-band absorber, utilizing spherical water resonators within the unit cell as absorbing elements. A strong and sharp absorption resonance is achieved at 3.38 GHz for a unit cell size of 15 × 15 mm². The surface demonstrates stability with respect to polarization, incidence angles up to 60°, and temperatures between 5°C and 45°C. Its operation is evaluated through simulations, with field images provided to offer insight into its performance.**

***Index Terms*—frequency selective surfaces, absorbers, all dielectric, electromagnetic compatibility, angle of incidence.**

I. INTRODUCTION

Frequency selective surfaces (FSSs) are passive or active two-dimensional periodic structures designed to control the parameters and propagation of electromagnetic waves in a meaningful way. They are used in applications such as antennas, reflectors and reflect arrays, screens and spatial filters, polarizers, absorbers etc. [1-3].

The design of FSSs typically involves metallic and dielectric materials, but innovative approaches incorporate novel materials such as graphene and liquid crystals. Purely dielectric solutions can withstand higher power levels, feature higher mechanical stability, and are suitable for higher frequencies, extending into the terahertz and optical domains, where the electromagnetic properties of metals differ from those at lower frequencies [4].

Various manufacturing techniques for producing and testing dielectric samples experimentally have been developed [5-10]. For example, additive manufacturing of all dielectric samples is reported in [7-9], and stereolithography for 3D printing is considered [5, 6, 10].

Absorbers consist of thin layers of stacked materials that operate in reflection mode, absorbing incident electromagnetic energy within specific frequency bands to minimize reflections. They are used in applications such as shielding enclosures and stealth technology. FSSs provide a favorable framework for absorber design [11].

Various authors [12-15] have explored water as a potential low-cost material for inclusion in FSS structures. Its use in absorbers has also been investigated due to the high imaginary component of its dielectric constant [2]. Additionally, the high real part of the dielectric constant enables miniaturization.

A transparent metamaterial absorber containing encapsulated water is described in [12]. Optical transparency is attained since the suggested absorber is made entirely of water and polydimethylsiloxane without the inclusion of any conductive patterns. 92.5% absorptivity has been obtained at 10.8 GHz when the proposed absorber is implemented with two layers, and it surpassed 90% in the 10.45–11.20 GHz region, or 6.9% bandwidth.

Paper [13] proposes and investigates broadband microwave absorbers using water-based metamaterial structure elements: water-droplet or water-tube. Water-tube design has achieved a significantly wide bandwidth from 5 GHz to 15 GHz for about 90% microwave absorption, and water-droplet design has achieved 90% microwave absorption from 7.5 GHz to 15 GHz. Both complete wave simulation and experimental testing have confirmed the broadband absorption performance.

The authors from [14] showed experimentally that their subwavelength water metamaterial exhibits absorption of over 90% across nearly the whole 12–29.6 GHz frequency range. Additionally, they demonstrated that the suggested metamaterial has good thermal stability, with its absorption capability remaining constant across the temperature range of 0 to 100°C. The metamaterial absorber's ability to function at broad angles of incidence is demonstrated by the examination of its angular tolerance.

This paper presents a cost-effective FSS design intended as a resonant water-based absorber. The unit cell consists of a readily available consumer-grade spherical container filled with water, with a metal ground plane on one side of the structure.

An electromagnetic CAD software is used to evaluate the reflection coefficients. The sensitivity of the design to temperature, polarization, and angle of incidence is examined.

This paper is organized as follows. The absorber's unit cell design is presented in Section II. The water-based absorber's electromagnetic response to incident electromagnetic waves is covered in Section III. Field images are used to gain insight into the operation of the absorber. The last section is dedicated to conclusions.

II. Unit Cell Design

The absorber is obtained by the periodic translations in the *x* and *y* directions of the unit cell, whose geometry is depicted in Fig. 1.

This unit cell contains a sphere of diameter *st* that is filled with water. The sphere resides in a Styrofoam container (ε_r=1.1, μ_r=1). The upper cover of the container is made of crown glass (ε_r=2.3, μ_r=1), which has been inserted for sealing the box. A metal layer is placed on the opposite face of the unit cell. The simulation software [16] requires the addition of air layers above and below the structure.

The metallic plate at the bottom of the structure has been simulated through an electric boundary condition. Metallic losses, which might enhance absorption, are neglected following this choice, leading to reflection coefficients potentially lower than those achieved with a true metal. Nevertheless, models with PEC run substantially more quickly than those containing actual metals, and it is known that dielectric losses are predominant [2].

The dimensions of the unit cell in the *xy* plane *dx* and *dy*, and the diameter of the sphere *st* have been subject to optimization. Debye 1st order model for water was used.

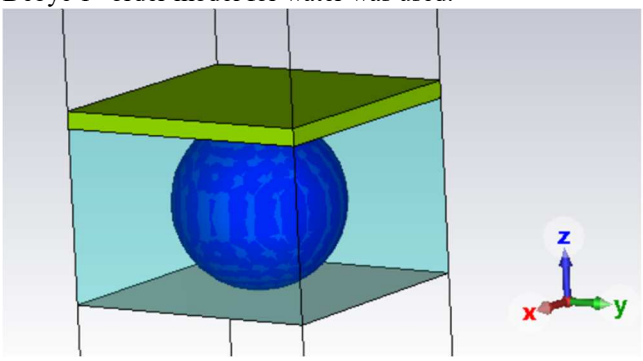

Fig. 1. Unit cell of the water-based absorber.

III. Water Absorber: Optimization and Operation

To simulate the electromagnetic response to incident plane waves, the frequency-domain solver of CST Microwave Studio (v.2024) [16] has been used. Unit cell (periodic) boundary conditions have been applied to the four boundaries along the *x* and *y* axes. Incident electromagnetic plane waves propagate in the negative *z* direction. The structure is bounded at the bottom by a metallic ground plane. A parametric analysis was carried out on the S_{11} parameter in the frequency range of 0 to 5 GHz, at a temperature of 20°C, in order to identify the optimized dimensions of the unit cell and the diameter of the sphere that produce the maximum reflection coefficient.

We started with *dx*=*dy*=40 mm, and the diameter of the sphere was parametrized between 20 and 35 mm. The result, visible in Fig. 2, depicts a large resonance at 1.69 GHz for *st*=20 mm (-25.48 dB reflection coefficient). Smaller resonances occur at 1.34 GHz. (for *st*=25 mm), 2.35 GHz (for *st*=30 mm) and 2.4 GHz (for *st*=35 mm).

Similarly, a parametric study was done for *dx*=*dy*=30 mm, by varying the diameter of the sphere between 10 and 25 mm this time. Fig. 3 indicates the occurrence of two resonances at 1.68 GHz (-11.18 dB) for *st*=20 mm and at 2.26 GHz (15.03 dB) for *st*=15 mm.

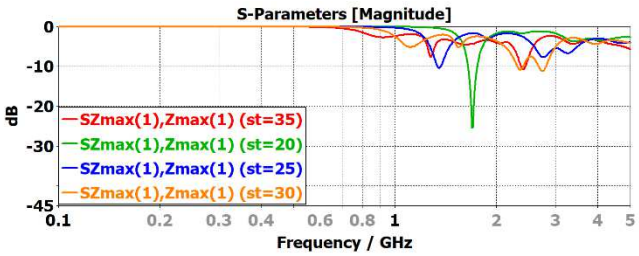

Fig. 2. Reflection coefficient of the absorber parametrized by several values of the diameter *st* of the water sphere (*dx*=*dy*=40 mm).

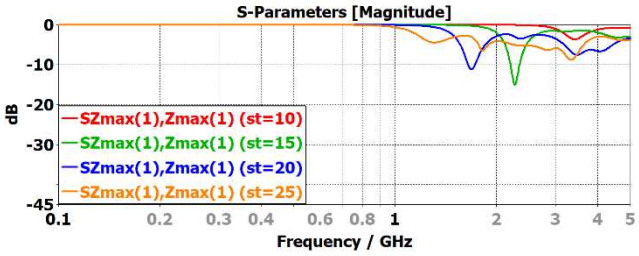

Fig. 3. Reflection coefficient of the absorber parametrized by several values of the diameter *st* of the water sphere (*dx*=*dy*=30 mm).

However, the best results are obtained by taking *dx*=*dy*=15 mm with a sphere diameter of *st*=10 mm, for which the reflection coefficient is -34.25 dB at a resonance frequency of 3.38 GHz, according to the results shown in Fig. 4. The frequencies of 3.19 and 3.68 GHz are the -10 dB stop-band limits. Consequently, this particular diameter value was selected for all the following investigations.

However, it is worth mentioning that resonant notches below -10 dB appeared at frequencies between 2.7 and 4.4 GHz, for all values of the diameter between 8 and 14 mm, giving designers more options in design.

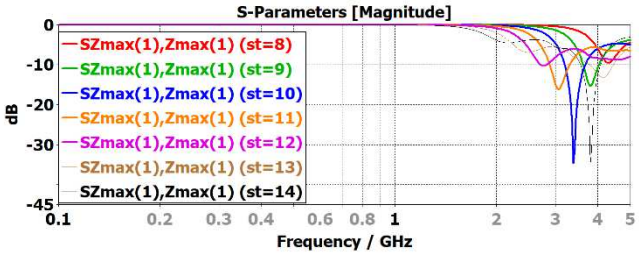

Fig. 4. Reflection coefficient of the absorber parametrized by several values of the diameter *st* of the water sphere (*dx*=*dy*=15 mm).

The promising results obtained for normal incidence of electromagnetic plane waves upon the structure must be confirmed by testing the absorber's response to obliquely incident waves. Due to the structure's symmetry, we calculated only the variation of the reflection coefficient with the incidence angle (angle of the wavevector with the *z* axis) [2]. However, since the geometric layouts of TE and TM modes differ, both must be taken into account.

For the TE mode, Fig. 5 shows the reflection coefficients

computed for a parametric variation of the incidence angle θ in steps of 15 degrees, between 0 and 60°. Consistency and polarization insensitivity up to 60° are demonstrated by the results. The reflection coefficient varies from -36.53 dB at 15° to -11.82 dB at 60°, however the notch stays centered at 3.38 GHz.

Fig. 6 shows that the similar parametric analysis that was performed for the TM scenario. The consistency is identical for the same variation in the incidence angle θ as in the TE case. Namely, as θ varied from 0 to 60 °, the resonance frequency shifted from 3.38 GHz to 3.56 GHz, with associated reflection coefficient values of -34.79 and -21.22 dB, respectively. As a result, the water absorber functions efficiently up to a 60° incidence angle.

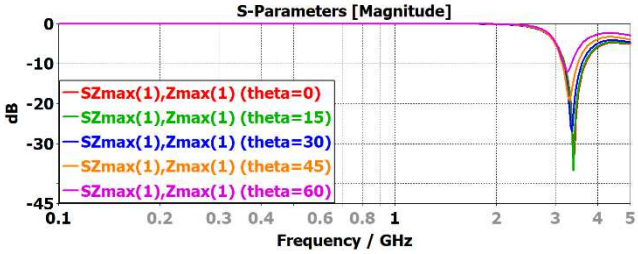

Fig. 5. Reflectance of the water absorber parametrized by the incidence angle θ, at T=20°C (TE incidence).

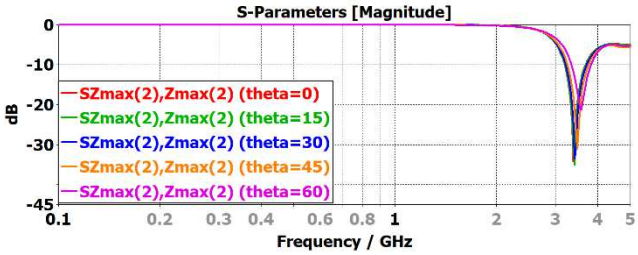

Fig. 6. Reflectance of the water absorber parametrized by the incidence angle θ, at T=20°C (TM incidence).

The simulations conducted so far assumed a water temperature of 20°C. Next, simulations were carried out in temperature increments of 5°C, from 5°C to 45°C in order to evaluate the possible variation of the frequency response when the absorber operates at different temperatures. Table I displays the results of these simulations together with the Debye model parameters (relaxation time and water's static and optical permittivity) that were employed.

One important finding is that, when temperature rises, the resonance frequency (fifth column) changes only slightly, ranging from 3.32 GHz to 3.59 GHz.

At the resonance frequencies the reflection coefficient (last column in Table I), ranges from -34.25 dB at 20°C to -12.98 dB at 5°C and -11.03 dB at 45°C. Although a noticeable variation occurs, the absorber performance is still adequate over the whole temperature range because the coefficient is still below -10 dB.

The electromagnetic field distribution inside the design must be considered in order to gain some insight into the physical process of the resonance in the water absorber.

TABLE I
THE WATER ABSORBER: DIELECTRIC CONSTANT, RESONANCE FREQUENCY AND REFLECTANCE

T (°C)	ε_s	ε_{inf}	τ ($\times 10^{-12}$ s)	f_{res} (GHz)	R_{res} (dB)
5	85.90	6.97	15.33	3.329	-12.98
10	83.95	6.74	13.00	3.359	-16.412
15	82.05	6.53	11.14	3.373	-21.96
20	**80.19**	**6.32**	**9.65**	**3.389**	**-34.257**
25	78.38	6.12	8.44	3.448	-24.27
30	76.61	5.93	7.43	3.478	-18.36
35	74.88	5.74	6.60	3.508	-15.00
40	73.19	5.57	5.91	3.547	-12.70
45	71.54	5.40	5.31	3.598	-11.03

Field images for the scenario of a normal incidence of the incoming wave in TE polarization (E||y) at a frequency of 3.38 GHz and a temperature of 20°C are shown in Fig. 7 and Fig. 8. Because of the structure's symmetry, the results for TM polarization (E||x) are identical to those oh the TE normal incidence case. These figures depict the electric field in the plane x=0, and the magnetic field intensity respectively, at the resonance frequency (with a phase difference of 90° between them).

A magnetic dipole resonance occurs in the water area, as seen by the vortex created by electric field lines from Fig. 7. Electric boundary conditions at the ground plane cause the field lines to be perpendicular to the ground.

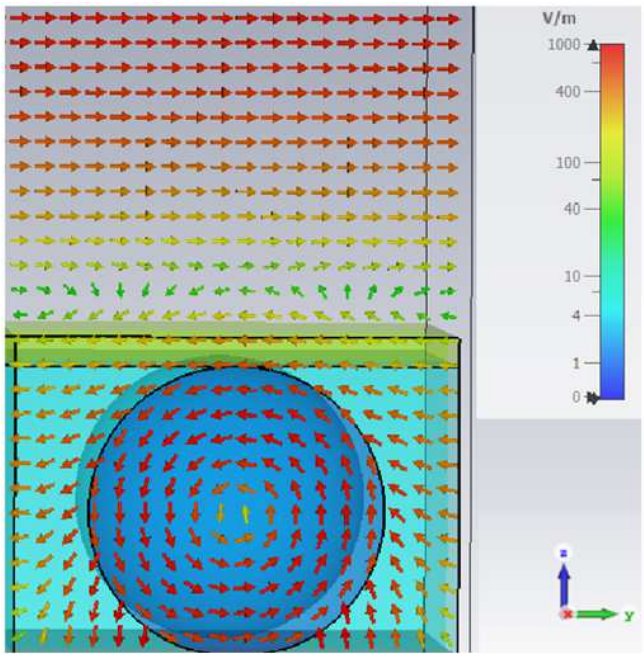

Fig. 7. Electric field intensity at f= 3.38 GHz, in TE incidence (E||y).

A strong magnetic field intensity that is perpendicular to the vortex and parallel to the x axis is confirmed by Fig. 8. We deduce that a magnetic resonance is associated with the water absorption frequency in the present situation.

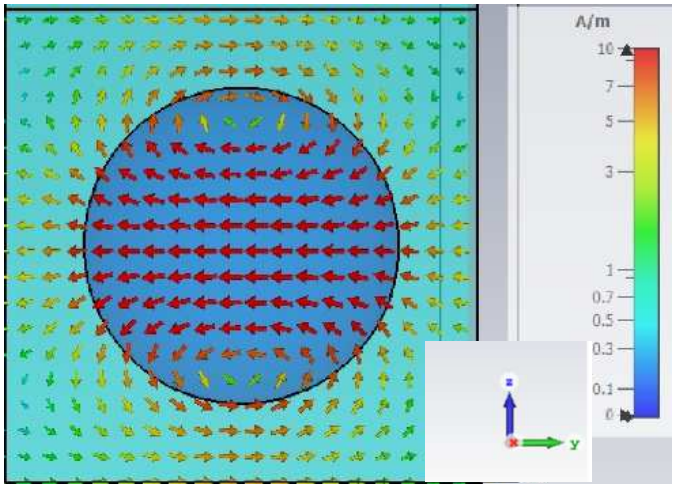

Fig. 8. Magnetic field intensity at f= 3.38 GHz, in TE incidence (E||y).

IV. Conclusions

An FSS capable of operating as a water-based absorber has been designed and analyzed. The unit cell's geometric dimensions have been optimized to achieve notch resonance. Electromagnetic CAD software has been used to simulate and evaluate the absorption characteristics of the proposed structure. The absorber's operation is explained using field images.

At 3.38 GHz, the water absorber's reflection coefficient showed a deep and sharp resonance. Stability of the notch has been demonstrated up to an incidence angle of 60°, and the resonance frequency displayed temperature stability in the 5–45°C range.

Future research will concentrate on creating tunable absorbers with liquid circulation systems and using different liquids to adjust the resonances.

References

[1] B. A. Munk, Frequency Selective Surfaces: Theory and Design, NJ: Wiley, pp. 1-10, 2000. doi:10.1002/0471723770.

[2] A. De Sabata, A. Silaghi, C. Ionica, O. Pacurar, "Design of Liquid Based Frequency Selective Surfaces Operating as Absorbers," Advances in Electrical and Computer Engineering, vol.24, no.4, pp.75-82, 2024, doi:10.4316/AECE.2024.04008.

[3] A. Buta, A. Silaghi, A. De Sabata, L. Matekovits, "Multiple-Notch Frequency Selective Surface for Automotive Applications", 2020 13th International Conference on Communications (COMM), 18-20 June 2020, Bucharest, Romania, 2020. doi:10.1109/COMM48946.2020.9142001.

[4] J. Wang, S. Qu, L. Li, J. Wang, M. Feng, H. Ma, H. Du, Z. Xu, "All-dielectric metamaterial frequency selective surface", J. Adv. Dielectr., Vol. 7, Nr. 5 (2017), 1730002-1--1730002-11, 2017. doi:10.1142/S2010135X1730002Xt.

[5] J. H. Barton, C. Garcia, E. Berry, R. Salas, R. Rumpf, "3-D Printed All-Dielectric Frequency Selective Surface With Large Bandwidth and Field of View", IEEE Trans. Antennas Propag., Vol. 63, No. 3, March 2015. doi:10.1109/TAP.2015.2388541.

[6] J. H. Barton et al., "All-dielectric frequency selective surface for high power microwaves", IEEE Trans. Antennas Propag., Vol. 62, No. 7, pp. 3652–3656, July 2014. doi:10.1109/TAP.2014.2320525.

[7] R. Mellita, S. Karthikeyan, P. Damodharan, "Additively Manufactured Conformal All-dielectric Frequency Selective Surface", 2020 50th European Microwave Conference (EuMC), 12-14 January 2021, Utrecht, Netherlands, 2021. doi:10.23919/EuMC48046.2021.9338224.

[8] D. Z. Zhu, M. D. Gregory, P. L. Werner, and D. H. Werner, "Fabrication and characterization of multiband polarization independent 3-D-printed frequency selective structures with ultrawide fields of view", IEEE Trans. Antennas Propag., vol. 66, no. 11, pp. 6096–6105, November 2018. doi:10.1109/TAP.2018.2866507.

[9] J. Zhu, Y. Yang , D. McGloin , S. Liao , Q. Xue, "3-D Printed All-Dielectric Dual-Band Broadband Reflectarray With a Large Frequency Ratio", IEEE Trans. Antennas Propag., Vol. 69, No. 10, pp. 7035-7040, October 2021. doi:10.1109/TAP.2021.3076528.

[10] S. Young et al., "Additively-Manufactured All-Dielectric Microwave Polarization Converters Using Ceramic Stereolithography", IEEE Open Journal Antennas Propag., Vol. 4, pp. 339-348, March 2023. doi:10.1109/OJAP.2023.3257355.

[11] A. De Sabata, O. Lipan, L. Matekovits, A. Silaghi, "Comparison between frequency selective surfaces with rectangular and hexagonal periodicity operating as absorbers," 2023 International Conference on Electromagnetics in Advanced Applications (ICEAA), 9-13 October 2023, Venice, Italy, 2023. doi:10.1109/ICEAA57318.2023.10297723.

[12] Q. Wang, K. Bi, S. Lim, "All-dielectric transparent metamaterial absorber with encapsulated water," IEEE Access, Vol. 8, pp. 175998- 176004, September 2020. doi:10.1109/ACCESS.2020.3026358.

[13] J. Zhao, et al., "Broadband microwave absorption utilizing waterbased metamaterial structures," Opt. Express, vol. 26, no. 7, pp. 8522–8531, April 2018. doi:10.1364/OE.26.008522.

[14] J. Xie et al., "Water metamaterial for ultra-broadband and wide-angle absorption," Opt. Express, vol. 26, no. 4, # 318885, February 2018. doi:10.1364/OE.26.005052.

[15] A. Andryieuski, S. M. Kuznetsova, S. Zhukovsky, Y. Kivshar, A. Lavrinenko, "Water: Promising Opportunities For Tunable All-dielectric Electromagnetic Metamaterials", Sci. Rep. 5:13535, Aug. 2015

[16] CST Microwave Studio, v. 2024, www.3ds.com.